63. Carew, D. P. and Staba, E. J., *Lloydia*, 1965, **28**, 1.
64. Al-Abta, S., Galpin, I. J. and Collin, M. A., *Plant Sci. Lett.*, 1979, **16**, 129.
65. Turnbull, A., Galpin, I. J., Smith, J. L. and Collin, H. A., *New Phytol.*, 1981, **87**, 257.
66. Collins, H. A. and Watts, M., in *Handbook of Plant Cell Culture*, vol. 1, (eds Evans, D. A., Sharp, W. R., Ammirato, P. V. and Yamada, Y.), Macmillan Publ. Co, New York, 1983, p. 729.
67. Lindsey, K. and Yeoman, M. M., in *Primary and Secondary Metabolism of Plant Cell Culture* (ed. Neumann, K. H.), Springer-Verlag, Berlin, 1985, p. 304.
68. Townsley, P. M., *J. Inst. Can. Sci. Technol. Alim.*, 1974, **7**, 76.
69. Ravishankar, G. A., Rajasekaran, T. and Venkataraman, L. V., in *Proc. Natl. Symp. on Recent Advances in Plant Cell Tissue Culture of Economically Important Plants* (ed. Reddy, G. M.), Osmania University Press, Hyderabad, 1988, p. 119.
70. Diomande, M., *ATAS Bull. Tissue Culture*, 1984, p. 26.
71. Horowitz, R. M. and Gentilli, B., *US Patent*, 1983, **3**, 87.
72. Purhan, Z. and Martin, S. W., *Prog. Ind. Microbiol.*, 1971, **9**, 13.
73. Persions, G. J., *US Patent*, 1973, **3**, 723, 410.
74. Morris, J. A., *Manuf. Confect.*, 1972, **52**, 38.
75. Tahara, A., *Kegaku Kogyo*, 1972, **23**, 398.
76. Tahara, A., *Yakugaku Zasshi*, 1973, **93**, 951.
77. Handro, W., Hell, K. G. and Kerbau, G. E., *Planta Med.*, 1977, **32**, 115.
78. Furuya, T., in *Frontiers of Plant Tissue Culture* (ed. Thrope, T. A.), University of Calgary, Calgary, Canada, 1978, p. 191.
79. Arup, S., *Biotechnol. News*, 1989, **9**, 5.
80. Mathew, A. G., Lewis, Y. S., Jagadishan, R., Nambudiri, E. S. and Krishnamurthy, N., *Flavour Ind.*, 1971, **2**, 23.
81. Yeoman, C. M. M., Miedzybrodzk, M. S., Lindsey, K. and Mclaunchlna, W. R., in *Plant Cell Culture: Results and Perspectives* (eds Sala, F., Parisi, B., Cella, R. and Giferri), Elsevier, New York, 1980, p. 327.
82. Ravishankar, G. A., Venkataraman, L. V. and Kadyan, A., *Curr. Sci.*, 1988, **57**, 679.
83. Ravishankar, G. A., Rajasekaran, T., Sarma, K. S. and Venkataraman, L. V., in *Proc. Symp. Plant Cell and Tissue Culture of Economically Important Plants* (ed. Reddy, G. M.), Osmania University, Hyderabad, 1987, p. 110.
84. Sujata, V., Ravishankar, G. A. and Venkataraman, L. V., *Appl. Biochem. Biotechnol.*, 1990, **12**, 336.
85. Watanabe, K., Yano, S. and Yamada, Y., *Phytochemistry*, 1982, **21**, 513.
86. Pais, M. S. *et al.*, in *VI Int. Congr. Plant Tissue and Cell Culture* (eds Somers, D. A., Gengenbach, B. G., Biesboer, D. D., Hackett, W. P. and Green, C. E.), IPATC, USA, 1986, p. 69.
87. Ravishankar, G. A., Rajasekaran, T. and Venkataraman, L. V., *Pyrethrum Post*, 1989, **17**, 66.
88. Shannon, J. C. and Garwood, D. L., in *Starch: Chemistry and Industry* (eds Whistler, R. L., Paschall, E. F. and BeMiller, J. N.), Academic Press, New York, 1984, p. 26.
89. Lawrence, R. H., *Cereal Foods*, 1987, **32**, 759.
90. Flavell, R. B., Payne, P. I., Thompson, R. D. and Law, C. N., *Biotech. Bioengg. News*, 1984, **2**, 157.
91. Kunimoto, L., *Biotechnology*, 1986, **40**, 58.
92. Sharp, W. R., *J. Am. Oil Chem. Soc.*, 1986, **63**, 594.
93. Fujita, Y., Hara, Y., Suga, C. and Morimoto, T., *Plant Cell Rep.*, 1981, **1**, 61.
94. Tisserat, P., *Biotechnology*, 1987, **5**, 10.
95. Himeno, H. and Sano, K., *Agric. Biol. Chem.*, 1987, **51**, 2395.

RESEARCH ARTICLE

A computer simulation model for action potential in an excitable membrane

Minal P. Mujumdar and Chanchal K. Mitra
School of Life Sciences, University of Hyderabad, Hyderabad 500 134, India

We present a computer simulation of action potential, developed in most cell membranes but a characteristic property of the neuron membrane. The simulation program is a model developed theoretically to see the generation of action potential once the nerve is stimulated, using values from the literature and calculated values. The effects of different factors, such as rate of diffusion, slopes of the permeability curves used to determine the permeability of the different ions, and strength of the external stimulus applied, on the action potential are also seen. The best-suited values for better results are then chosen. The basic interest is to study, theoretically, the various aspects of action potential generation and the restoration of resting potential, and to compare the results with those of experimental studies.

IN a living cell a potential difference exists between the cytoplasm and the extracellular environment, with the inside of the cell generally being negative with respect to the outside. This potential is called resting potential and is caused by the unequal distribution of ions in the inside and outside solutions on either sides of the plasma membrane surrounding the cell and by differences in ionic permeabilities. The neuron membrane is capable of generating a nerve impulse (transient potential change) and has a unique structure, the synapse, for transferring information from one neuron to another, when stimulated.

When the nerve impulse starts, after having been triggered, the voltage across the membrane is lowered locally. Immediately ahead of the electrically altered region (in the direction in which the nerve impulse is propagated) channels in the membrane open and let Na^+ ions pour into the axon.

The process is self-reinforcing: the flow of Na^+ ions

through the membrane opens more channels as there is a possibility of pore interaction[1], which makes it easier for more Na^+ ions to flow. The Na^+ that enter change the internal potential of the membrane from negative to positive. Soon after the sodium channels open, they close, and another group of channels open that let K^+ ions flow out. This restores the voltage inside the axon to the resting value. The sharp positive and negative charge that show up as a 'spike' is known as the 'action potential' and is the electrical manifestation of the nerve impulse. A more detailed background on the biophysics of the excitable membranes is found elsewhere[2-5].

This brief description of the nerve impulse illustrates the importance of ion channels and ion fluxes for the electrical activity of neurons or membranes in general. Thus understanding the diffusion of ions is a fundamental aspect in action potential studies and has been a subject of concern to physiologists and biophysicists. We thought computer simulation of the biological model of the ion diffusion across membranes would be of more approximation to the living model and would be useful for both analytical and numerical solutions in this field. The simulation model although involves few assumptions, arbitrary parameters and choosing a form of function to fit the experimental data available, it gives a overall picture of the phenomenon under experiment.

In this paper we report a computer simulation model for the action potential generation in membranes in general, considering the diffusion across the membrane and in the bulk solutions, the permeabilities of the channels to the movement of different ions and the active pump effects. We also report the effects of different stimulus strength on the so obtained action potential spikes through the simulation model. As mentioned earlier, we have arbitrarily chosen a few values and also taken few values from the literature in the simulation. This may associate the work with arbitrariness but lets the fundamental ideas remain the same and lets us understand the basics of the biological model and the mathematical calculations governing the membrane excitation systems that are very fascinating.

A simulation on the Hodgkin Huxley model has already been worked out by Wheal[6] but this is quite different from our model.

Model description (method of simulation)

Diffusion

The diffusion is considered to follow Fick's diffusion laws and the axon is considered, for this simulation, a flat plate with two sides corresponding to the two sides (viz. inside and outside) of the axon. The channel is considered as a small 'pore' that allows flow of ions with a rate that depends on the permeability of the ion considered (which in turn depends on the potential) and the concentration gradient. The diffusion across the pore and the bulk solutions inside and outside are considered independently. The diffusion from and to the bulk of the solution to the 'pore' takes place, for the computational purposes, in imaginary layers that have adjustable thickness. To compute the concentrations of various ionic species in various layers, we use Fick's second law

$$\frac{dc}{dt} = D \cdot \frac{d^2c}{dx^2}$$

in the spherical polar coordinate system this becomes

$$\frac{dc}{dt} = D \cdot \left[\frac{d^2c}{dr^2} + \frac{2}{r} \cdot \frac{dc}{dr}\right].$$

This form of the Fick's law was used for the numerical computations. We considered 200 imaginary layers (hemispherical, centered around the 'pore') and made use of the above equation. The diffusion coefficient was replaced by a dimensionless constant, ALPHA.

For the diffusion across the 'pore', we made use of Fick's first law. The fluxes of various ions (Na^+, K^+ and Cl^-) were calculated:

$$J = D \cdot (C_{out} - C_{in}).$$

The flux of ionic species cannot be treated as independent particles as their flux is determined both by concentration gradient and electrical forces generated by all the ions present and hence the flux was calculated by using the following formula[7]:

$$J = P \cdot e^s/(1 - e^s) \cdot (C_{out} - C_{in} \cdot e^s)$$

where s = POT·Z·F/RT; POT, membrane potential; Z, charge on the ion; F, Faraday constant; R, gas constant; T, temperature; P, permeability coefficient; C_{in}, inside concentration of the ion; C_{out}, outside concentration of the ion.

Concentration changes in the first layer were calculated from this equation. Again, another dimensionless constant ARC was introduced which takes into consideration the effective value of P.

In the simulation thus, two dimensionless constants, ALPHA and ARC were introduced for numerical convenience. The time axis, given in the graphs, depends on the choice of the dimensionless constants. These two constants are defined below:

$$\text{ALPHA} = \frac{D \cdot dt}{(\Delta r)^2}$$

$$\text{ARC} = \frac{D \cdot A \cdot dt/dx}{(2/3) \cdot \pi (\Delta r)^3}.$$

Here, D is the diffusion coefficient for the ions (potential-free), Δr the thickness of the imaginary layers

considered, dt time interval for each iteration loop, A area of the 'pore' and dx thickness of the 'pore'.

The ratio of the two constants, i.e. ALPHA/ARC, is another dimensionless constant, and is given by $(2/3)\cdot\pi\cdot\Delta r\cdot dx/A$. This ratio controls the relative rates of the bulk diffusion and the diffusion across the 'pore'.

Another algorithm is introduced which calculates the final rate of diffusion, taking into consideration the effect of fixed charges on the diffusion rate of the ions. This module also takes care that the electroneutrality is maintained during the diffusion across the pore.

Permeabilities

The permeabilites of the Na^+ and the K^+ ions were calculated by using an integral form of the Lorentzian equation that shows a sigmoidal pattern. For the Cl^- ion, the permeability is kept constant at a constant value (0.4 in the simulations presented). In the resting membrane, the permeabilities are in the ratio of $P_{Na}:P_K:P_{Cl}=0.04:1:0.4$ whereas in the active membrane (at the peak of the action potential) the ratios[8] are 20:1:0.4. The permeabilities are potential and electrochemical gradient-dependent. We have considered only potential dependence. The permeability function used in the simulation is of the following form which is empirical:

$$P=\frac{P_{max}}{\pi}[\tan^{-1}(y\cdot(\text{potential}-\text{offset}))+\pi/2].$$

Here P_{max} is the maximum value of the permeability suitably chosen (20 and 1 for Na^+ and K^+ respectively). The offset is empirically adjusted to give the rising portion of the permeability at a suitable potential

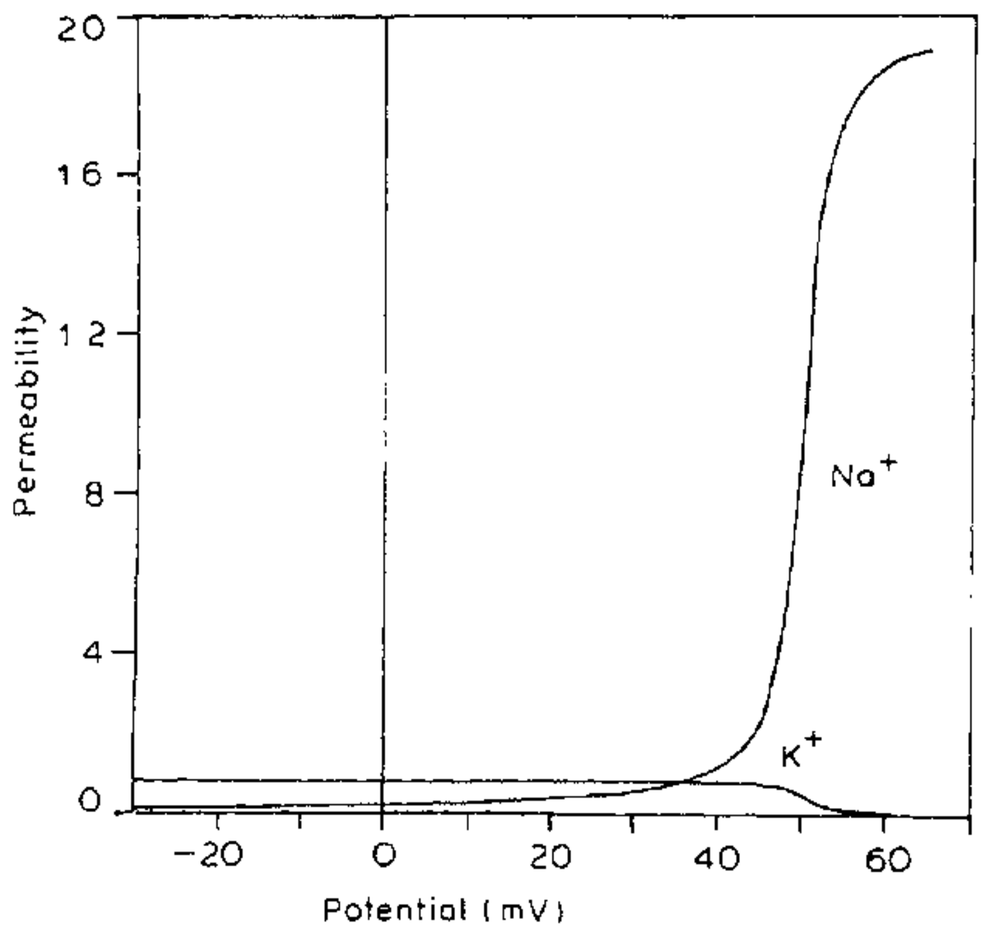

Figure 1. Sodium and potassium permeability as a function of potential. The maximum permeability for sodium is 20 and that for potassium is 1. The offset is taken as 50 mV.

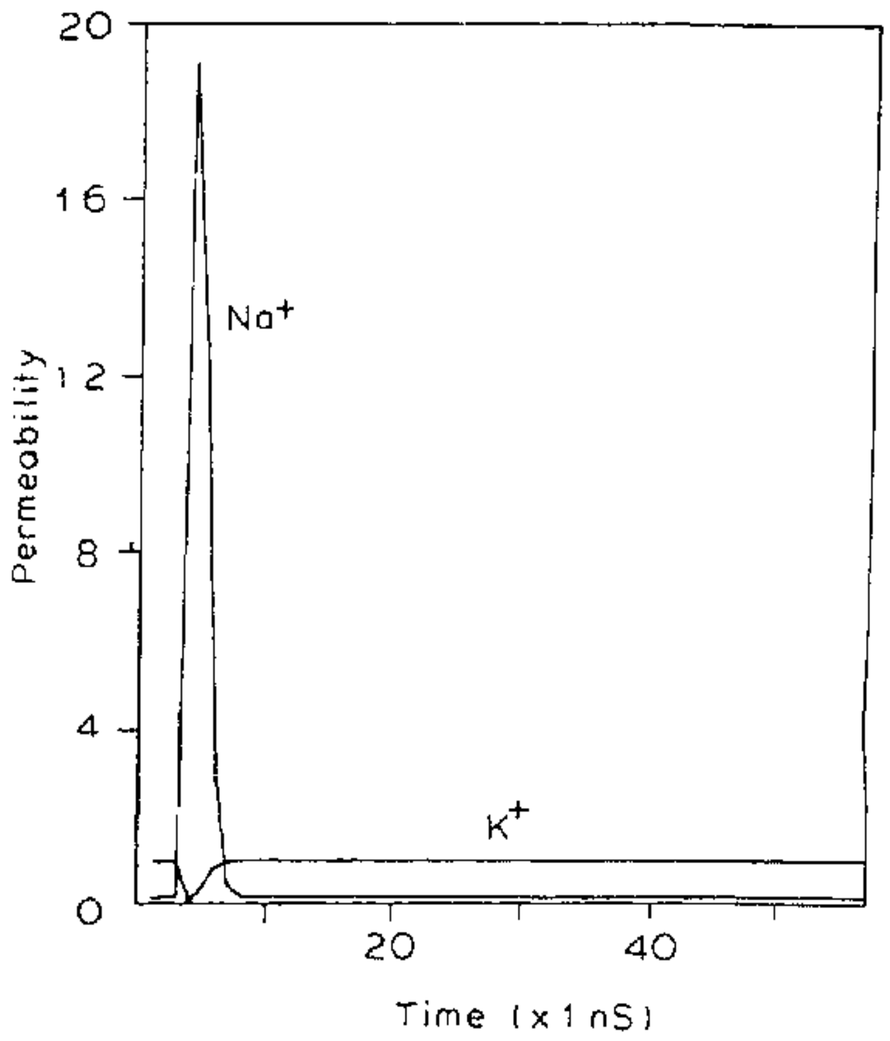

Figure 2. Relative changes for sodium and potassium during the course of action potential.

(50 mV in our case). Again, y is another adjustable parameter suitably chosen to produce a reasonable slope of the permeability curve (0.5 in our case). The equation is slightly modified for K^+ permeability calculation ($P=\pi-P$ for K^+), which gives a decrease in the K^+ with increasing potential. The permeability for K^+ also follows sigmoidal curve as we consider that there exists different conformational states of the channel during opening and closing.

Figure 1 shows the variation of the Na^+ and K^+ permeabilities used in our present simulation with potential. Figure 2 shows the variation of permeability with time as the action potential is generated. The permeability is calculated with the permeability equation for every iteration for Na^+ and K^+. The calculated values are then plotted against the iteration number. The X-axis plots only the first 100 iterations as the rest of the simulation gives the maintainance of the resting potential.

Potential

We have found Goldman–Hodgkin–Katz (GHK) equation[9] to represent satisfactorily the potential of the membrane under non-steady conditions. However, we have also tried other equations, viz. the Chang equation[10], but the differences are apparently not significant. The equation used is:

$$\text{POTential}=\frac{RT}{F}\ln\frac{P_{Na}[Na_0]+P_K[K_0]+P_{Cl}[Cl_i]}{P_{Na}[Na_i]+P_K[K_i]+P_{Cl}[Cl_0]}$$

$$=59\log\frac{P_{Na}[Na_0]+P_K[K_0]+P_{Cl}[Cl_i]}{P_{Na}[Na_i]+P_K[K_i]+P_{Cl}[Cl_0]}.$$

This form is valid only in the resting potential condition, when the sum of all charges carried by ions through the membrane is zero, but under active state the current carried due to diffusion of ions must be accounted for, which therefore makes it important to derive the equation of potential which incorporates an additional term $C \cdot RT/\mathrm{POT} \cdot F$, where C is calculated in every iteration, in the GHK equation and so the modified GHK equation we used was as follows:

$$\mathrm{POTential} = 59 \log \frac{P_{Na}[Na_0] + P_K[K_0] + P_{Cl}[Cl_i] + V}{P_{Na}[Na_i] + P_K[K_i] + P_{Cl}[Cl_0] + V}$$

where $V = C \cdot RT/\mathrm{POT} \cdot F$ and C, net current flowing across the membrane calculated in every iteration.

The concentration values are taken to be that of the first layer on the appropriate side. The resting state inside concentrations for Na^+, K^+ and Cl^- taken were 50, 400 and 70 mM respectively and the outside concentrations were taken as 460, 20 and 540 mM respectively[11].

Active pump

The potential will also depend upon the turnover of the Na^+–K^+-ATPase since this pump is not electroneutral. The pump was simulated by a simple algorithm in which the concentrations were forced to remain equal to the concentrations in the resting state. This is somewhat arbitrary and to some extent erroneous, but the results indicate that if the concentrations in the 5th layer (or some other small value) is forced to remain close to the bulk concentrations, diffusion can adequately bring back the potential to the resting value in a short time.

Results

Computing and running the program has given the following results:

The simple diffusion of Na^+, K^+ and Cl^- without the consideration of the fixed immobile charges on either sides of the membrane shows that the concentration tends to become equal on both the sides and equilibrium is restored which is not the case in the living systems. However if the effect of fixed charges is considered, the system tends to return to the resting potential and the graphs obtained are as is seen in Figure 3. Concentrations of the different ions, Na^+, K^+ and Cl^-, at the end of the simulation also confirm this fact as they are close to the original concentrations.

The base line at -45 mV in Figure 3 is obtained when no stimulus is applied. The resting potential in the first iteration is set to -45 mV by calculating the potential, using the permeability values from our calculation in the GHK equation.

Application of stimulus of different strengths at the third iteration gives the graphs shown in Figure 3. Like in the living systems the simulation also follows the same rules of stimulation, i.e. below a threshold, the spike obtained is not very significant which cannot be propagated and above the threshold whatever be the strength of stimulus applied, it produces the same amplitude of action potential (spike height). Thus the threshold range for this particular system is 55–59 mV.

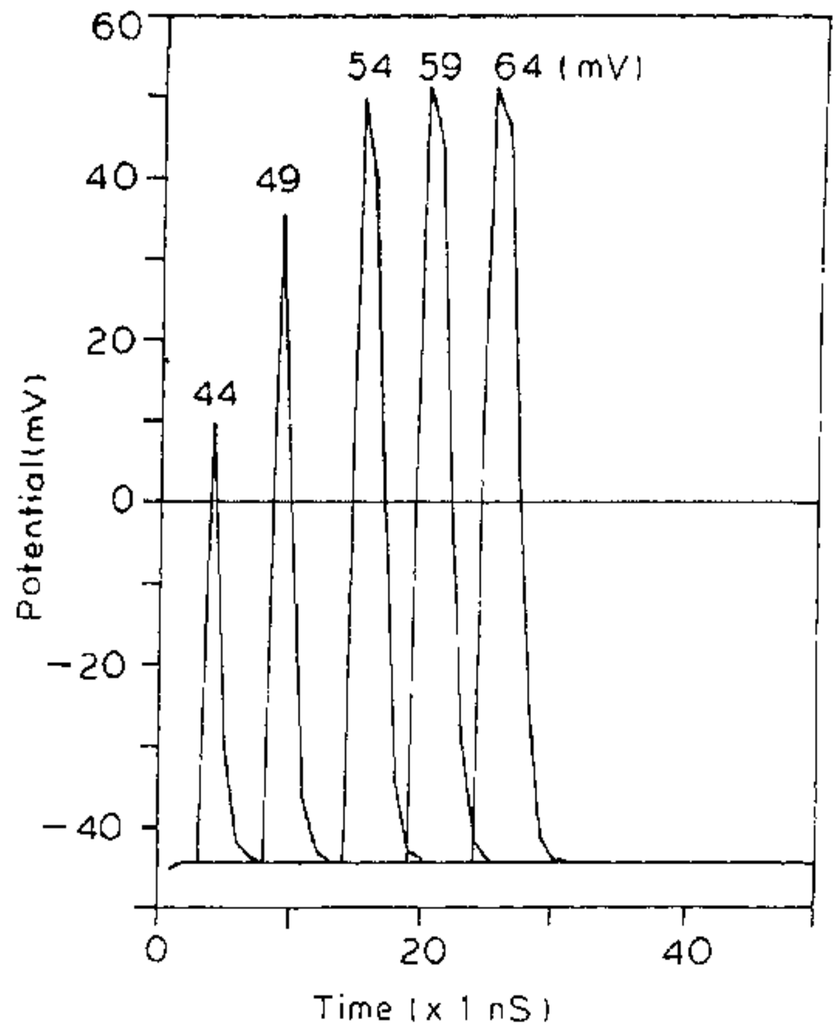

Figure 3. Effect of stimulus strength on the action potential. The curves have been shifted by 5 units successively along the X-axis for visual clarity.

Rate of diffusion (ROD) at the particular iterations during the spike generation and the resting potential restoration is plotted against time in the similar way as potential is plotted (Figure 4). There is a sudden and considerable change in the ROD of Na^+ during spike generation which is also the case in the living systems. Similar is the case with Cl^- which shows a deviation of approximately 11 (arbitrary) units from the resting state value as the diffusion of Cl^- is taken to be dependent on the diffusion of Na^+ and K^+ for electroneutrality consideration. Thus electroneutrality has been assumed (via Cl^- movement) during Na^+ or K^+ fluxes. In the absence of electroneutrality, the potential at any point of time will depend on the ionic current and the membrane capacitance. The K^+ ROD shows a deviation of one unit. The figure clearly shows the maximum ROD values of K^+ and Na^+ during different time durations, that is the maximum Na^+ ROD is attained during the rising phase of the action potential spike whereas maximum K^+ ROD value is attained during the fall of the potential to the resting value. The concentrations of the different ions, Na^+, K^+ and Cl^- can also be plotted in the similar way but the scales

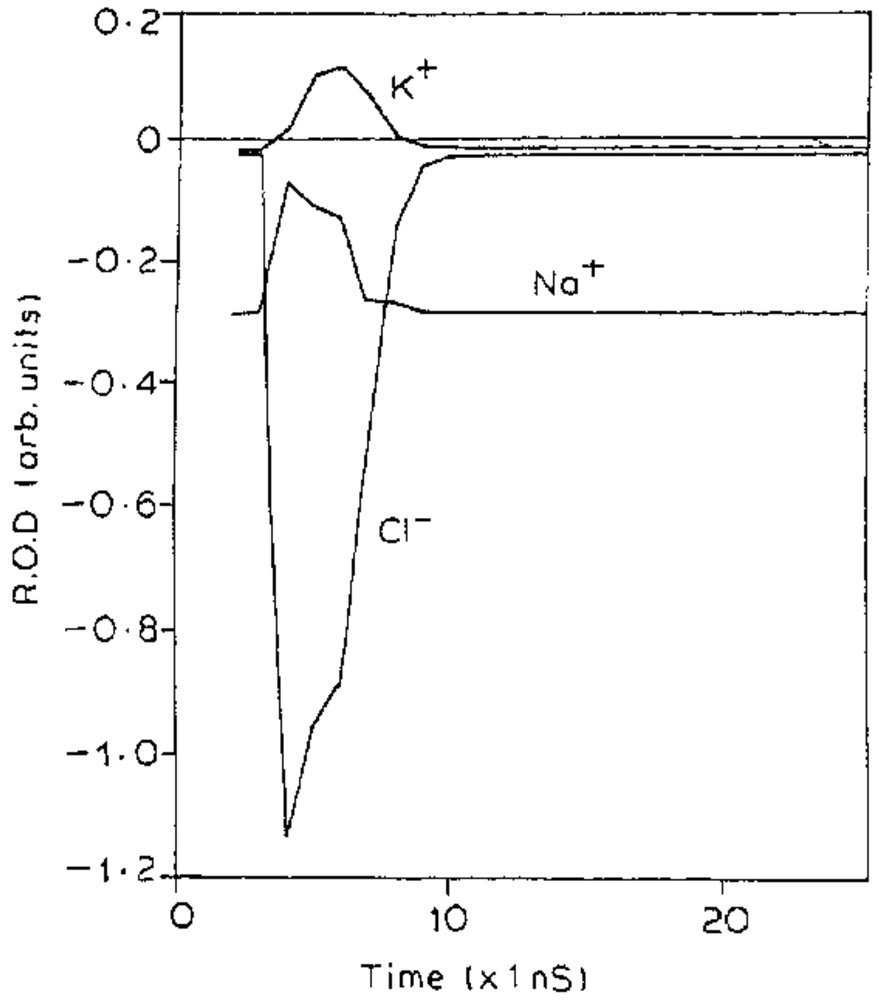

Figure 4. Rate of diffusion of the various ions during the course of action potential.

being widely distributed and the change being for a short duration a small change in the concentration cannot be distinguished and hence the ROD graphs were looked into as it gave a better view.

The effect of changing values of ALPHA and ARC, the diffusion coefficient constants in our program for that in the imaginary layers on the sides of the membrane and that for across the membrane respectively, also was checked. Changes in these values apparently change the rate of diffusion. The ratio of the two dimensionless constants apparantely affects the time duration of each iteration, so we fixed their values for having a particular time scale.

Changes in the y parameter value in the permeability equation used in the simulation virtually changes the slope of the sigmoidal graph and has direct effect on the potentials of the system. The pattern of the graph so obtained from different values of y remains the same. For our calculations, y value of 0.5 gave the desired potential amplitude and resting potential.

Discussion

Simple calculations of the permeabilities of Na^+ and K^+ that follow a sigmoidal pattern graph can govern the potential of the membrane. This might be because the sigmoidal pattern takes into consideration the different states of conformation, the channel undergoes during its opening and closing[12] and thus gives better results rather than the linear pattern.

The diffusion of the ions, namely Na^+, K^+ and Cl^- no doubt is responsible for the action potential generation but the effect of immobile charges cannot be ignored as they affect the diffusion of the former ions. This is something like the Donnan membrane potential in the living systems.

Application of different strength of stimulus on the simulated system showed the similar results as would be in the real systems, following the rules of the stimulation.

The ROD graphs from simulation also confirm the fact that during the rising phase of the action potential, there is a sudden increase in the Na^+ permeability across the membrane and once the peak is obtained its permeability slowly declines and thereafter the membrane becomes more permeable to K^+.

In all, our simulation model obeys the important rules of membrane excitation and is therefore a good method to study the problem theoretically.

Simplified description of the method, merits and limits

Through our simulation model, we try to generate action potential under artificial conditions and compare its properties to those developed in the living systems, mainly considering the neuron membrane. The model helps us to understand the theory behind the action potential generation which is mainly caused by a sudden change in the permeability of the membrane to the different ions during the process, diffusion of the ions across the membrane, the effect of immobile charges and the effect of active pumps on the resting potential restoration. The model takes into account only the voltage gated channels and the effect of the nonexcitable channels[13] is not considered. The propagation of the action potential brought about by the chemically gated channels, present generally in the synaptic region, is not included in the simulation model.

The program takes into account several variable parameters to which we have given arbitrary values and so the model may appear arbitrary which is actually not the case as the values taken have some mathematically calculated background. The active pump effect considered in the program is just direct without considering the means by which the ions are transported back to the resting state conditions. The different means so involved and the factors affecting the active pumps[14] are still under our investigation.

1. Liebovitch, Larry, S. and Fischbarg, J., *J. Theor. Biol.*, 1986, **119**, 287.
2. Hodgkin, A. L. and Huxley, A. F., *Proc. R. Soc. London*, 1958, **B148**, 1.
3. Hodgkin, A. L. and Katz, B., *J. Physiol.*, 1949, **108**, 37.
4. Keynes, R. D., *J. Physiol.*; 151, **114**, 119.
5. Huxley, A. F., *Science*, 1964, **145**, 1154.
6. Wheal, H. V., *J. Physiol.*, 1985, **364**, 23.

7. Macey, Robert I., in *Membrane Physiology* (eds. Thomas E. Andreoli; Joseph F. Hoffman and Darrell D. Fanestil), Plenum, New York, 1980, pp. 137–139.
8. Meves, H., *Curr. Top. Membr. Transp.*, 1984, **22**, 279.
9. Goldman, D. E., *J. Gen. Physiol.*, 1943, **27**, 37.
10. Chang, Donald, C., *Biophys. J.*, 1983, **43**, 149.
11. Bruce Alberts, *et al.* (eds.), *Molecular Biology of the Cell*, Gradland Publishing Inc., New York, 1983, pp. 286–302.
12. Armstrong, Clay, M. and Matteson, Donald, R., *Curr. Top. Membr. Transp.*, 1984, **22**, 331.
13. Chang, Donald, C., *Biophysics. J.*, 1986, **50**, 1095.
14. Mullins, L. J., in *Membrane Transport in Biology*, Vol. II, (ed. Tosteson, D. C.), Springer-Verlag, Berlin, 1979, pp. 161–208.

ACKNOWLEDGEMENTS. We thank CSIR, New Delhi, for financial assistance.

6 December 1989; revised 12 July 1990

ESR study of Cu(II): thiostrepton complex

C. Vasant Kumar Chary*, C. R. N. Sarma and S. Rambhav†
Bhavan's New Science College, Narayanguda, Hyderabad 500 029, India
†Department of Biochemistry, University College of Science, Osmania University, Hyderabad 500 007, India

Thiostrepton (MW 1650) forms a stable complex with Cu(II) in 1:4 molar ratio with total loss in its biological activity. The *g* values of the metal ion obtained from the ESR spectra of the complex in powder and in different solvents at room temperature and at liquid nitrogen temperature (LNT) indicated a well co-ordinated metal ion with the ligand. Large exchange interactions between the Cu(II) ions present well within the complex molecule in the powder and in the liquid resulted in a single symmetric resonance line, while the LNT spectra are resolved in some of the solvents. The interacting and non-interacting nature of these solvents with the complex and the probable stereo structure of the ligand around the metal ion in one of the solvents are discussed.

CHELATING properties of certain antimicrobial agents with metal ions enable a broad understanding about the mode of their action, especially when metal chelation affects their biological activity. Chelation with metal ions may result in either enhancing, stabilizing or abolishing the bioactivity of these agents[1–3]. Various mechanisms are explained for such altered activities of these antimicrobial agents on interaction with the metal ions[3]. Therefore, metal chelation of antibiotics has been the subject of intense investigations[4–7].

The molecular structure of thiostrepton, a peptide antibiotic[8], (Figure 1) reveals that it has many sites at which metal coordination can occur. Therefore in our studies on the structure–activity correlations of thiostrepton, the effect of metal ion interaction on its biological activity was investigated. While these studies along with spectroscopic characterization of the antibiotic molecule in the metal complexes using UV, CD, IR and NMR constitute a major part of our investigations, here, we report the ESR study of Cu(II): thiostrepton complex.

Thiostrepton (MW 1650) was a gift sample from The Squibb Institute, New Jersey, USA. All the solvents used were of analar grade and used directly. UV spectra were recorded on Beckman's DU–50 recording spectrophotometer. ESR spectra were recorded on Brucker X-band spectrometer at 9.71 GHz. The spectra were analysed using manganese (Mn^{2+} in MgO) and DPPH as the standards. The error in $g_{\parallel}$ and $A_{\parallel}$ values reported is ± 0.006 and $\pm 9 \times 10^{-4}\ cm^{-1}$ respectively. The centre field in all the spectra was maintained at 3200 G (indicated by an arrow mark in the figures).

Thiostrepton (165 mg, 0.1 mmol) was dissolved in 1,4 dioxane (5 ml). To this solution, $CuCl_2 \cdot 2H_2O$ (1 g) dissolved in water (1 ml) was added and thoroughly mixed. The reaction mixture was then incubated at 37°C for 24 h. To the resultant mixture, dioxane (200 ml) was added gradually with constant stirring. A light-green-coloured product was precipitated on standing. The precipitate was collected by centrifugation and washed successively with dioxane and ether and finally dried *in vacuo*. Yield 112 mg. The purity of the complex was ascertained by thin layer chromatography using different solvent systems. UV absorption of the complex was recorded in 20% dimethylsulphoxide (DMSO). The biological activity of the complex was determined by the method as described earlier[9].

Powder complex (6 mg) was digested on a sand bath with 5 ml of perchloric acid:nitric acid mixture (5:1 v/v). Later, the residue was dissolved in 3 ml of water and its metal content was estimated by flame photometry using a Perkin-Elmer atomic absorption spectrophotometer.

The ability of thiostrepton to complex with Cu(II) was also determined by the modified continuous variation method of Job[7] as follows: To 0.25 ml of thiostrepton solution (0.06 μmol) in DMSO were added 0.1, 0.15, 0.2, 0.3, 0.4, 0.5, 0.6, 0.8 and 1.0 ml of copper

*For correspondence.